E-7797

NASA Technical Memorandum 106128

Low Earth Orbital Atomic Oxygen Environmental Simulation Facility for Space Materials Evaluation

Curtis R. Stidham and Thomas J. Stueber
Sverdrup Technology, Inc.
Lewis Research Center Group
Brook Park, Ohio

Bruce A. Banks, Joyce A. Dever, and Sharon K. Rutledge
National Aeronautics and Space Administration
Lewis Research Center
Cleveland, Ohio

and

Eric J. Bruckner
Cleveland State University
Cleveland, Ohio

NASA

LOW EARTH ORBITAL ATOMIC OXYGEN ENVIRONMENTAL SIMULATION FACILITY

FOR SPACE MATERIALS EVALUATION

Curtis R. Stidham and Thomas J. Stueber
Sverdrup Technology, Inc.
Lewis Research Center Group
Brook Park, Ohio 44142

Bruce A. Banks, Joyce A. Dever and Sharon K. Rutledge
National Aeronautics and Space Administration
Lewis Research Center
Cleveland, Ohio 44135

and

Eric J. Bruckner
Cleveland State University
Cleveland, Ohio 44115

ABSTRACT

Simulation of low Earth orbit atomic oxygen for accelerated exposure in ground-based facilities is necessary for the durability evaluation of space power system component materials for Space Station Freedom (SSF) and future missions. A facility developed at the National Aeronautics and Space Administration's (NASA) Lewis Research Center provides accelerated rates of exposure to a directed or scattered oxygen beam, vacuum ultraviolet (VUV) radiation, and offers in-situ optical characterization. The facility utilizes an electron-cyclotron resonance (ECR) plasma source to generate a low energy oxygen beam. Total hemispherical spectral reflectance of samples can be measured in situ over the wavelength range of 250 to 2500 nm. Deuterium lamps provide VUV radiation intensity levels in the 115 to 200 nm range of three to five equivalent suns. Retarding potential analyses show distributed ion energies below 30 electron volts (eV) for the operating conditions most suited for high flux, low energy testing. Peak ion energies are below the sputter threshold energy (~30 eV) of the protective coatings on polymers that are evaluated in the facility, thus allowing long duration exposure without sputter erosion. Neutral species are expected to be at thermal energies of approximately .04 eV to .1 eV. The maximum effective flux level based on polyimide Kapton mass loss is 4.4×10^{16} atoms/cm²•s, thus providing a highly accelerated testing capability.

1. INTRODUCTION

Spacecraft operating in the low Earth orbital (LEO) environment must be designed to withstand the effects of solar radiation (particle and electromagnetic), micrometeoroid and space debris impacts, deep thermal cycles, plasma interactions, and neutral atomic oxygen (AO). Atomic oxygen and ultraviolet radiation are cited as the environmental constituents that cause the most damage to the chemistry of polymeric surfaces (1). Atomic oxygen is the predominant species in the LEO environment between the altitudes of 180 and 650 kilometers and results from the photodissociation of molecular oxygen by solar ultraviolet radiation (2). In the thermosphere, atomic oxygen and ions are present at thermal kinetic energies of approximately .1 eV. The relative velocities of spacecraft with respect to the plasma environment (~7.2 Km/s) causes the kinetic

1

energy of the atomic oxygen impacting spacecraft surfaces, normal to ram, to be sufficiently energetic (approximately 4.5 eV) to break many chemical bonds (3). Materials such as organic polymers are readily oxidized while some metals form protective oxide layers. The synergistic effects of atomic oxygen, thermal cycling and ultraviolet radiation exposure may contribute to the performance degradation of space power system components. Degradation can occur in mechanical and electrical properties as well as surface optical properties such as solar absorptance and thermal emittance, which are important to the thermal control of low temperature radiators and other system components. Changes in these properties will result in penalties on component performance and, therefore, require LEO environmental durability evaluation prior to utilization in space application. These evaluations can be performed on shuttle flight experiments, but this can be cost and time prohibitive. Thus, in addition to flight evaluation, reliable, accelerated ground-based testing facilities are needed to provide cost effective and timely evaluations of materials and components. Proper correlation between ground-based systems and flight results are required for meaningful durability evaluation.

A facility for the simulation of the LEO environment has been developed at the NASA Lewis Research Center (LeRC) to investigate the effects of the LEO environment on spacecraft materials. This facility is designed to evaluate either the effects of atomic oxygen on materials or the synergistic effects of simultaneous VUV radiation and atomic oxygen exposure. Initially designed in the mid-1980's the facility has undergone numerous engineering changes, these previous configurations are described in references 4 and 5. The objective for the facility has been to develop accelerated simulation capabilities that will reliably predict the performance of materials and power system components in the LEO environment. Currently, the facility can be configured to provide accelerated rates of atomic oxygen exposure to a large area directed oxygen beam or scattered isotropic atomic oxygen arrival, by means of an ECR plasma source. Both configurations can be operated simultaneous with vacuum ultraviolet (VUV) radiation, controlled sample heating, and in situ reflectance characterization. This paper describes the facility with its various operational modes and the analysis techniques used to characterize the exposure conditions.

The energy of the oxygen species present in the oxygen beam are at thermal energies (neutrals) or have a distributed energy less than 30 eV (ions) and therefore are not the same as the on-orbit ram energy of 4.5 eV. The interpretation of environmental durability results from the ECR plasma source requires care and this subject has been presented in detail elsewhere (6). For the sake of completeness, a brief discussion on the probability of reaction as a function of energy is included in Section 4 of this paper.

2. LEO ATOMIC OXYGEN ENVIRONMENTAL SIMULATION FACILITY

2.1 Vacuum Facility The vacuum chamber used for this facility measures 71 cm in diameter by 1.71 m long. The vacuum pumping system consists of a 25.4 cm, 6100 l/s diffusion pump, backed by a 115 l/s roots-type blower and a 1520 l/min rotary vane pump. All pumps are operated on perfluorinated ether (Fomblin) oil. The pumping system maintains a base vacuum pressure below 8.0×10^{-2} Pa with an oxygen gas flow into the ECR plasma source of 50 standard cm^3/min (SCCM). The facility utilizes a programmable logic controller (PLC) for automated vacuum control. In addition, the PLC is used to provide fail safe operation by monitoring the ECR microwave power supply, the electromagnets' power supplies and numerous permissives, including gas and water flows, and a microwave leak detector. The PLC provides protection to both the facility operator and the test subjects, thus guaranteeing testing integrity.

2.2 Electron Cyclotron Resonance Plasma Source Atomic oxygen simulation is achieved in the facility with the utilization of a 1000 watt ECR plasma source to generate a low energy, broad area beam consisting of atomic oxygen, ions, radicals, and metastables. The ionic oxygen is estimated by the manufacturer to represent approximately 1/10 of the species present in the plasma source (7). The ECR plasma source system is shown in the side view schematic of the facility (figure 1a). An oxygen plasma is generated midway

down the source chamber and flows out the quartz chamber liner (14 cm I.D.) into the exposure chamber, with the charged species following the potential path setup by the electrons moving down the magnetic field lines. The plasma is generated from the ionization, dissociation, and excitation of molecular oxygen due to electron collisions. For a 2.45 GHz microwave, the electron-cyclotron resonance condition occurs at a magnetic field strength of 875 gauss. At this position in the source the microwave energy is resonantly absorbed by the plasma electrons (8). Typically, the objective is to maximize the flux to accelerate testing, therefore the source is operated at maximum power and gas flow. Since the charged species follow the magnetic field lines, the lower magnet can be used to increase the ion current density at the sample site.

Samples can be exposed, with proper fixturing, from the end of the source liner to the bottom of the chamber, across an 18 cm diameter test area. Typically, samples are mounted at a distance of 45 cm from the liner in the plane of operation for the computer controlled positioning system and the rotating sample plate which are discussed later. Unless otherwise noted, the 45 cm position is the location for the discussion of sample exposure and beam characterization. The oxygen beam arrival to the samples can be configured in two general modes of operation. These two modes are directed beam and scattered isotropic atomic oxygen arrival.

2.2.1 Directed Arrival Directed beam arrival is the mode of operation used for highly accelerated rates of atomic oxygen exposure. Atomic oxygen acceleration rates based on Kapton effective flux measurements range from 31 and 122 times (for a ram orbit at SSF altitudes), depending on the distance from the source.
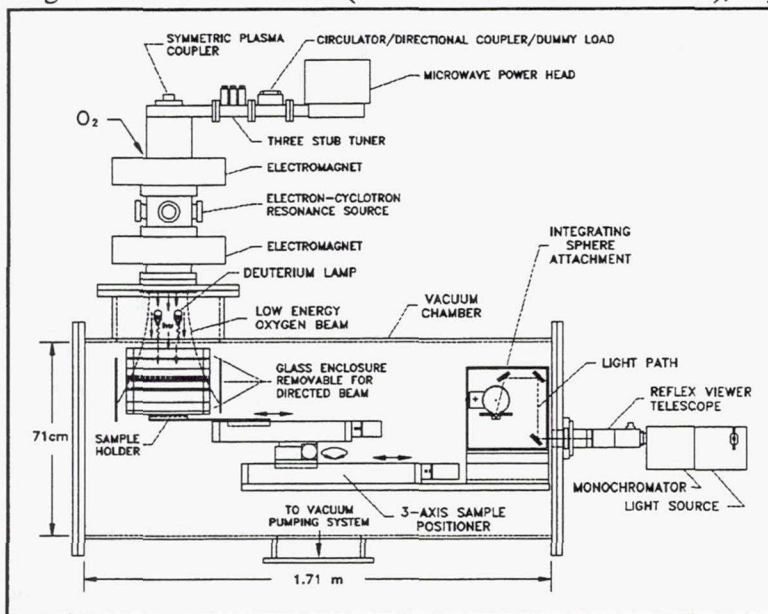

Figure 1a: Side View Schematic

The ion flux for this mode of operation is 9.00×10^{14} ions/cm$^2 \cdot$s, determined by planar button probe measurements (see Section 3.1.2). The energy of the neutrals at the sample site are expected to be at thermal energies on the order of 1×10^{-2} to 1×10^{-1} eV. This energy comes from the creation of the plasma in the source liner. Characterization of the energy of the neutral species has not been determined experimentally in this facility. The energy of the ionized species has been experimentally determined, with the use of a Retarding Potential Analyzer (RPA) probe, to be a dual distribution with peaks occurring at 10.5 and 25 eV (Section 3.2).

2.2.2 Scattered Isotropic Arrival The isotropic arrival mode of operation is achieved by scattering the expanding oxygen beam off of fused silica fixtures. The fixturing consists of a triangular fixture that is centered in the beam and its base is normal to beam arrival. The triangle's interior is lined with aluminum foil to provide VUV and UV radiation blockage for the samples underneath. The remaining fixture consists of a pair of outer glass surfaces and two end plates used to contain the diverging beam. This configuration is represented in the schematic of the facility (figures 1a-b) and is shown in the photograph of the facility (figure 2). This fixturing was originally introduced to the facility to provide VUV radiation protection to

samples that are sensitive to this intense radiation. The ECR source is expected to produce intense radiation at 130 nm, the resonance line spectra of atomic neutral and singly ionized oxygen. This subject is presented in more detail in Section 3.4.

This mode of operation forces some of the oxygen ions and neutrals in the beam to have at least one collision with a glass panel before reaching the sample site. Since the flux is highest at the center of the beam, a large majority of the beam constituents should have multiple collisions (off the center triangle and side panels) and become thermally accommodated to the temperature of the glass fixturing. The collisions should also serve to neutralize part of the ions in the beam and thus decrease the ion current density and increase the neutral population. Results from ion current density measurements show that the current density for the scattered configuration was half that of the directed exposure (see Section 3.1.2). The ion flux for this mode of operation is 3.26×10^{14} ions/cm$^2 \cdot$s (see Section 3.1.2). The Kapton effective flux was approximately 3.7×10^{15} atoms/cm$^2 \cdot$s (see Section 3.1.1) . The energy of both the charged and neutral species, that have collisions with the glass fixturing, is expected to thermally accommodate to an energy of $\sim .04$ eV. The pressure in the fixturing region is expected to be higher than the base pressure, resulting in short mean free paths. As a result, gas collisions may occur that prevent collisions with the glass fixturing thus resulting in energies higher than that of full thermal accommodation. The ion energy distribution measured for this configuration showed a single distribution with a peak energy at 7 eV (Section 3.2).

2.3 Vacuum Ultraviolet Radiation   The VUV lamps used for the synergistic atomic oxygen/VUV exposure configuration are 30 W deuterium lamps with magnesium fluoride windows. They are installed at a distance to provide approximately three to five equivalent suns in the wavelength range between 115 and 200 nm. The lamps are mounted in the upper portion of the vacuum chamber outside of the oxygen beam and positioned such that they are directed toward the sample exposure region (figures 1a-b). A pair of lamps is used to uniformly illuminate the 5 cm by 14 cm sample holder area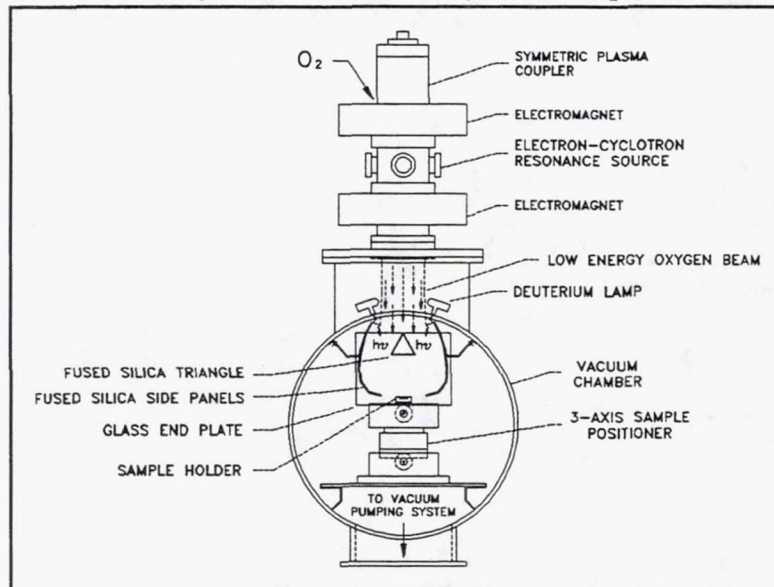. A PLC is used to control the operation of the lamps and provides a time history of operation for each lamp. These lamps have an average lifetime of approximately 300 hours. Therefore, for longer exposures, it is necessary to have additional lamps available to continue exposure in the event that a lamp burns out. Two pairs of lamps are installed in the facility for this reason. If a lamp in one pair burns out, the PLC turns off the remaining lamp in that pair and sends a signal to turn on the second pair to continue the VUV illumination of the samples without interrupting the test. If a lamp in this second pair fails, the PLC will determine whether a diagonal pair, one lamp from each set, is available and, if so, will send a signal to illuminate that diagonal pair. If a diagonal pair is unavailable, the PLC

Figure 1b: End View Schematic

will continue to illuminate the samples with the single lamp already on and upon its expiration, the PLC will turn on the single remaining lamp to continue the exposure. The PLC can also be used to cycle the lamps on and off during testing to provide prescribed levels of VUV exposure relative to the atomic oxygen exposure level. This provides the ability to correlate atomic oxygen fluence and VUV exposure for a particular spacecraft on-orbit environment.

2.4 Reflectance Measurement System   The Reflectance Measurement System (RMS) provides the facility with the capability of measuring in situ total hemispherical spectral reflectance of opaque samples over the wavelength range of 250 to 2500 nm, from which solar absorptance is calculated. The RMS utilizes a spectrophotometer specifically configured for use in this facility (figure 1a). A focusable monochromatic beam is produced outside of the vacuum chamber by the combination of a quartz halogen source assembly, monochromator, and a reflex viewer telescope that is used to focus and align the monochromatic beam at the sample site. The monochromatic beam is directed through a quartz feedthrough window and into an integrating sphere attachment which is inside of the vacuum chamber. The beam of light which strikes the sample positioned against the integrating sphere wall is at 10° off normal. An aperture is used at the monochromator exit to reduce the beam size so that it is smaller than the sample port opening of 1.9 cm (3/4") diameter. Two detectors are used to cover the wavelength range of this system. They are mounted on a sliding stage that is a part of the integrating sphere attachment thus providing the ability to manually change detectors during the scan with a linear push-pull feedthrough.
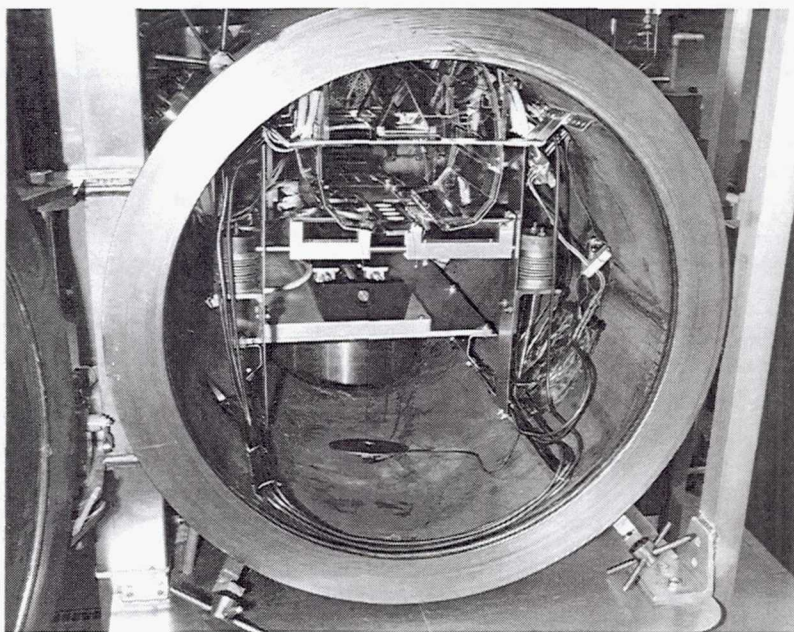

Figure 2: Photograph (Facility End View)

An IBM compatible computer is used with software provided by the manufacturer for automatic scanning. The software controls the wavelength drive unit of the monochromator and receives data from the detectors. During a scan, the software prompts the user for necessary adjustments to the equipment such as detector and grating changes. Data can be taken at wavelength intervals which are multiples of 5 nm. The user can set the desired noise level (0.5%, 1%, 2% or 5%) for a scan and the system will obtain sets of three readings at each wavelength until they agree within the prescribed noise level.

This is a single beam system and, therefore, requires that a reference material be scanned prior to scanning a sample. The program generates a conversion based on the measurement of the known reference and uses this to calculate the percent reflectance of the sample. The reference materials used are control samples of the samples being tested and therefore have similar surface reflectance characteristics. They are expected to be stable over the coarse of the test, because they are located in a position that is protected from the environment.

The sample holder for the RMS is capable of mounting up to four 2.54 cm diameter samples in a linear arrangement. The sample holder is mounted to a computer controlled three-axis positioning system that transports the samples between the AO/VUV exposure region in the chamber and the reflectance measurement port in the integrating sphere. The use of D.C. half-stepper motors on the two linear rails and the rotary stage provide accurate, highly repeatable sample positioning. A second holder mounted inside the integrating sphere attachment contains the two reference samples and an LED light source for the focusing and alignment of the telescope. This second holder is actuated manually via a linear push-pull feedthrough.

During AO/VUV exposure of the test samples, the light and sample ports in the integrating sphere attachment are sealed off with shutters thus protecting the internal Halon (PTFE) coating of the integrating sphere and the surfaces of the reference materials inside. The shutters are opened and closed manually with a linear push-pull feedthrough. Finally, the RMS is only operated when the ECR source and VUV lamps are shut off to prevent degradation of the materials in the integrating sphere attachment and to prevent electromagnet interference with the detectors.

2.5 Sample Heating Samples can be heated during testing using two different heating systems. For low temperature heating (below 130 °C), two quartz heater tubes are installed below the fused silica triangle used for beam scattering. The lamps are powered with a DC power supply and the temperature is controlled with a proportional-integrating (PI) controller. An IBM type compatible computer interfaced (via IEEE 488) with a scanning thermometer is used for temperature measurement providing a temperature time history for the test samples and the computer serves as a backup to the PI controller. The second heating system is a furnace for high temperature sample heating (below 600 °C). The ceramic heaters in the furnace are powered with a variable transformer and the outer wall of the furnace is water cooled.

2.6 Sample Articulation Samples can be mounted in a fixed configuration at different distances from the end of the ECR source liner. A rotary stage, driven by a stepper motor through a gear reduction box external to the chamber, oscillates samples ±180° during exposure for simulation of on-orbit sweeping atomic oxygen arrival such as would occur with articulation of a solar tracking array. The distance from the source liner can be adjusted with a chain-sprocket drive mechanism. Typically, it is operated at the 45 cm position coupled directly off of the end of the rotary feedthrough entering the chamber. Finally, a three-axis computer controlled position system is available for sample positioning. This system is an integral part of the RMS and was described in detail in Section 2.4.

3. CHARACTERIZATION OF SIMULATED LEO ENVIRONMENT

3.1 Oxygen Beam Flux Measurement The beam flux from the ECR source is determined by an effective flux measurement based on the mass loss of the material being tested, assuming in-space flight data exists on its erosion yield. If flight data is not available, polyimide Kapton H or HN is used to determine the effective flux since the in-space erosion yield is well known. This is an accepted standard of flux evaluation. The ion flux in the beam is determined with a planar button probe.

3.1.1 Effective Flux Measurement The effective flux measurement, based on mass loss, is calculated as follows:

$$Flux_{eff} = \frac{\Delta M}{\rho \times A_s \times t \times EY}$$

ΔM = Change in sample mass (g)
ρ = Density (g/cm^3)
A_s = Sample Area (cm^2)
t = Time (s)
EY = Erosion yield (cm^3/atom)

6

The in-space erosion yield for Kapton is 3×10^{-24} cm^3/atom based an atomic oxygen energy of 4.5 eV. Therefore, the flux calculated gives the equivalent in-space flux required to cause the same mass loss. The error on the flux measurements are typically $\pm 12\%$. The equivalent flux distribution has been determined for the directed and scattered arrival configurations at the 45 cm location and the directed configuration at 30 cm from the end of the source liner. For the directed configurations, the flux was determined across the 18 cm diameter test area. The flux distribution for the scattered arrival configuration was determined for the test area directly under the fused silica triangle used for beam scattering. The results are presented in table I along with the flux acceleration factors (Flux$_{eff}$/Flux$_{space}$) for ram, solar facing, and anti-solar facing orientations at SSF orbital altitudes.

Table I: Effective Flux Results and Acceleration Factors

Test Position / Measurement	Direct Arrival (30 cm)	Direct Arrival (45 cm)	Scattered Arrival (45 cm)
Flux$_{eff}$ Range (Atoms/cm^2•s)	3.9×10^{16} to 4.4×10^{16}	1.10×10^{16} to 1.45×10^{16}	3.35×10^{15} to 3.87×10^{15}
Flux Acceleration Factor for Ram: Flux$_{space}$ = 3.60×10^{14} (Atoms/cm^2•s)	108 to 122	31 to 40	9 to 11
Flux Acceleration Factor for Solar Facing: Flux$_{space}$ = 9.10×10^{13} (Atoms/cm^2•s)	429 to 484	121 to 159	37 to 43
Flux Acceleration Factor for Anti-Solar: Flux$_{space}$ = 1.14×10^{14} (Atoms/cm^2•s)	342 to 386	96 to 127	29 to 34

3.1.2 Ion Flux Measurement A planar button probe is used to determine the ion current density (ion flux) of the oxygen beam. The molybdenum button probe has a diameter of 1.115 cm and has a thin 100 nm gold sputtered coating to prevent surface oxidation. The probe is mounted in the chamber normal to the axis of the oxygen beam. A programmable electrometer with a built in voltage source is controlled by an IBM compatible computer via an IEEE 488 interface and is used for biasing the probe relative to ground potential and measuring the resulting current collected. A BASIC computer program is used for instrument control and data acquisition. The ion current density is determined by dividing the current collected by the probe's surface area. The current used to determine the ion current density is the potential at which the probe is sufficiently negative to retard electron arrival, this is typically -20 to -40 volts relative to ground. This potential can be determined by fitting a linear curve to the left straight line portion of the data on the curve and identifying the point at which the data starts to fall off of the line.
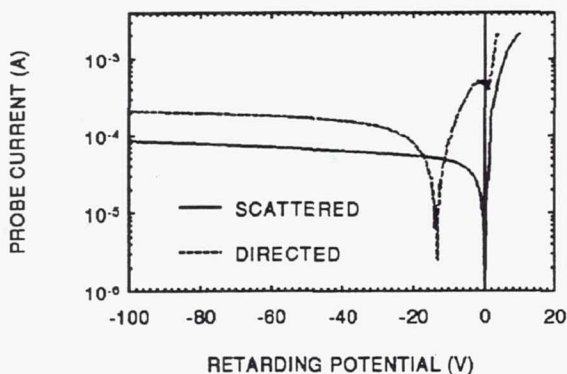

Figure 3: Button Probe Trace

The ion current density was determined for both the directed and scattered isotropic oxygen ion arrival configurations. The plot of the button probe traces for these two ion arrival configurations is shown in figure 3. The ion current density for the directed case was determined to be 1.44×10^{-4} A/cm^2 (flux = 9.00×10^{14} ions/cm^2•s) at a potential of a -37 volts. The ion current

7

density for the scattered case was determined to be 5.22×10^{-5} A/cm^2 (flux $= 3.26 \times 10^{14}$ ions/cm$^2 \cdot$s) at a potential of a -20 volts. Varying the voltage ± 5 volts from the potential used to determine these current densities results in a error in the measurement of approximately 5 percent.

3.2 Ion Energy Determination   The ion energy distribution of the oxygen beam is determined by using a Retarding Potential Analyzer (RPA) probe. The theory of operation of this type of electrostatic probe is presented by Kaufman (9). A two grid, single collector plate configuration is used to perform ion energy characterization. A schematic of the setup is shown in figure 4. The grids used in the probe are made of gold mesh having a mesh size of 39.4 wires/cm (100 wires/inch). The mesh is 80% transparent with a wire diameter of 2.54×10^{-3} cm (.001") and an opening space between wires of .227 mm (.009"). The collector plate is made of a 300 series stainless steel. The two grids are aligned in front of the isolated collector plate with the grids and collector plate equally spaced .208 cm (.082") apart. The first grid (the grid exposed to the
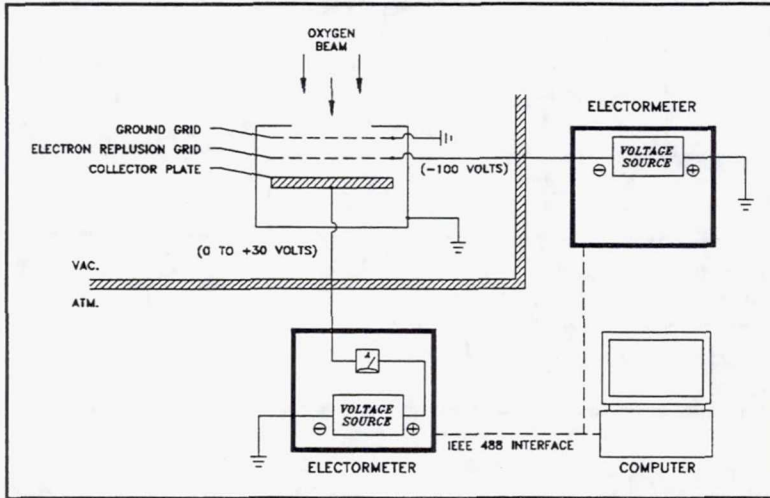

plasma) is electrically grounded and the second grid is typically biased -100 volts relative to ground potential. The second grid is the electron repulsion grid and the first grid is in place to prevent the potentials within the RPA from affecting the arriving ion and electron flux. The electron repulsion potential that will be used during a probe sweep is determined to be the potential where a negligible change in current exists on the collector plate, with the plate at ground potential, as the potential on the repulsion grid is decreased to eliminate electron arrival. During the RPA test, the ion collector plate is swept through a potential range of 0 volts up to 30 to 40 volts, in

Figure 4: RPA Schematic

increments of .2 volts. The upper limit for the sweep is determined based upon the negligible change in current witnessed on the collector plate (on the order of 1 μA) with an incremental increase in its potential, while the electron repulsion grid is biased.

Two programmable electrometers are used for the RPA tests. The electrometers are controlled by an IBM compatible computer via an IEEE 488 interface. A BASIC computer program is used for instrument control and data acquisition. One of the electrometer's voltage source is used to bias the electron repulsion grid and the other electrometer is used to bias the collector plate and measure the ion current collected. A commercial software package is used to provide polynomial regression curve fitting to the I-V data collected (figures 5a & 6a). For singly charged ions, plotting the absolute value of the derivative for this function over the swept voltage range results in the beam's ion energy distribution. The mean energy is calculated in the BASIC control program by determining the area under the I-V curve (Simpson's 1/3 Rule is used for the integration) and dividing by the current range ($I_{max} - I_{min}$).

The ion energy distribution from the ECR source was determined for the directed and scattered ion arrival configurations by computing the slope of the RPA collection current versus collection potential profiles. The energy was determined at a position of 45 cm from the end of the source liner with a gas flow of 50 SCCM. The RPA probe trace for the directed arrival configuration is shown in figure 5a. A dual distribution was observed with peaks occurring at 10.5 and 25 eV. The resulting energy distribution is shown in figure 5b.

The ion energy distribution was determined for the scattered ion arrival configuration. The RPA probe trace for this configuration is shown in figure 6a. The resulting energy distribution (figure 6b) has a single a peak

8

occurring at 7 eV. The existence of measurable ion fluxes at this RPA location, which does not allow line of sight ion arrival, is thought to be the result of ion collisions within the plasma that prevent some of the ions from colliding with the glass fixturing, and therefore preventing full neutralization by the glass fixture.
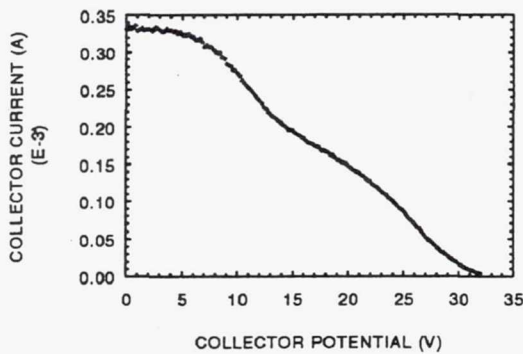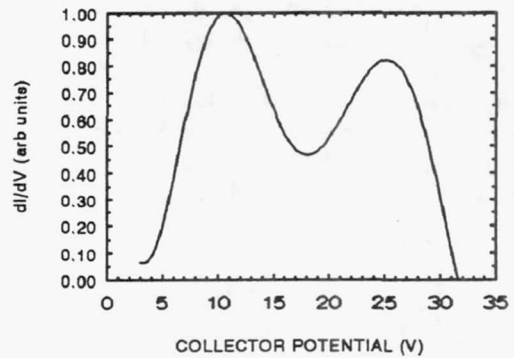

Figure 5a: RPA Probe Trace (Directed)

Figure 5b: Ion Energy Distribution (Directed)

Finally, the ECR is typically operated at 50 SCCM so to provide the largest possible flux. The advantage of this high flow is that with the increased pressure in the source the resulting ion energy is lowered (10).
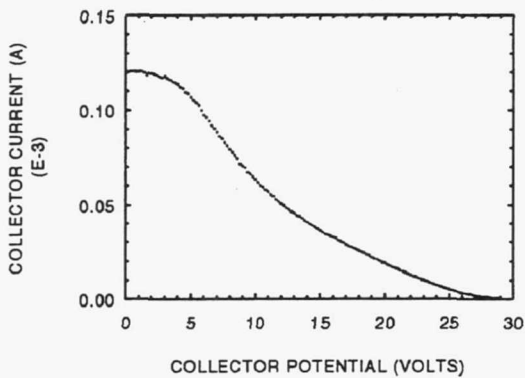

Figure 6a: RPA Probe Trace (Scattered)
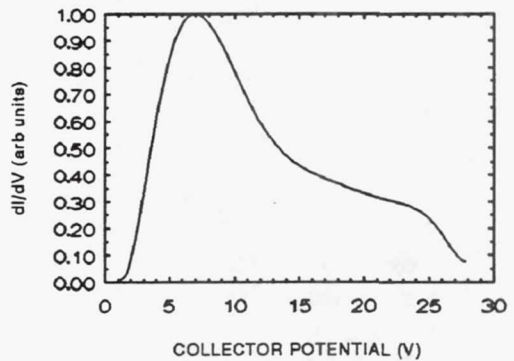
Figure 6b: Ion Energy Distribution (Scattered)

3.3 Deuterium Lamp Calibration   The deuterium VUV lamps are calibrated using a cesium iodide (Cs-I) photocathode to measure the integrated intensity between 115-200 nm. The Cs-I photocathode is used to measure the intensity of a lamp that has been calibrated by the National Institute of Standards and Technology (NIST) between 115-300 nm at 2 nm wide wavelength bands. A calibration factor is determined

9

for the Cs-I photocathode based on measurement of the standard VUV lamp. Lamps which are to be used for VUV exposure are measured with the calibrated detector. The distance is then determined at which a lamp will provide a desired number of VUV suns based on its intensity. The lamps are typically installed at distances so that they provide intensities of between three and five equivalent VUV suns.

3.4 ECR UV Radiation Measurement   A photomultiplier tube (PMT) coated with sodium salicylate was used with a set of narrow bandpass filters and a quartz diffuser window to obtain the UV content of the ECR source from approximately 180 to 400 nm. The PMT system was calibrated to a pyroelectric detector/radiometer system by measuring a mercury xenon short arc lamp with both systems at the same distance. The PMT system is much more sensitive than the radiometer, and the very low readings obtained with the PMT when measuring UV from the ECR source could not be correlated with equivalent radiometer readings. Therefore, it was assumed that the actual UV output of the ECR at each measured wavelength must be less than the minimum measurable radiometer readings at each of these wavelengths. The minimum radiometer readings, in all cases, corresponded to UV intensities of less than 0.2 suns based on the solar irradiance curve at air mass zero (11). This system; however, did not give information on vacuum ultraviolet radiation intensity which is expected to be intense, as occurs in radio frequency (RF) plasma ashers (12), particularly at the 130 nm characteristic resonance line for oxygen. Evidence of VUV radiation produced in the ECR plasma is the discoloration of zinc orthotitanate/potassium silicate thermal control coatings, which also occurs when exposed to an RF plasma asher (13).

4. DISCUSSION

The erosion yield of a material exposed to atomic oxygen is material and energy dependent, according to many investigators (6). The neutral atoms in the beam of the ECR plasma source are at energies estimated to be less than .1eV, therefore the probability of reaction and the erosion yield is less than in-space. The actual flux in the beam is much larger than the effective flux calculated, since the erosion yield is energy dependent. Calculations were made in an attempt to estimate the actual flux in the beam and the effect that the more energetic oxygen ions have on the erosion of Kapton. Since the erosion yield is energy dependent, estimates of erosion yield as a function of energy were made using Ferguson's model (Erosion Yield $\propto E^{.68}$) (14). The total mass loss of Kapton witness samples exposed in the facility were measured directly. The mass loss resulting from ion reaction was calculated based on the ion flux, ion energy distribution, and erosion yield of Kapton as a function of energy. The Kapton mass loss due to ions (assumed to be O^+) was calculated as follows:

$$\Delta M_{ion} = \left(\frac{j_i}{e}\right) \times t \times \rho \times A_s \times \int_{E_{min}}^{E_{max}} \frac{N(E) \times C \times E^{.68}}{\int_{E_{min}}^{E_{max}} N(E)\, dE}\, dE$$

e = electronic charge (1.6×10^{-19} coulombs)
j_i = Ion current density (A/m^2)
t = Time (s)
ρ = Kapton density (Kg/m^3)
A_s = Area of Kapton witness sample (m^2)
E = Energy (eV)
$N(E)$ = Relative number of ions at energy (E)
$C \times E^{.68}$ = Erosion yield of Kapton as a function of energy (14)
C = 1.079×10^{-30} (m^3/atom•$eV^{.68}$)

The relative number of ions $N(E)$ corresponds to the dI/dV curve from the ion energy distributions presented in Section (3.2). Subtracting the mass loss due to ions from the total mass loss gives the mass loss

10

due to the reaction of neutral oxygen. The neutral effective flux was then calculated using the equation for effective flux (Section 3.1.1). The actual neutral flux was calculated based on the probability of reaction for the thermal energy neutrals as followed:

$$Neutral\ Flux_{act} = (Neutral\ Flux_{eff}) \times \frac{Probability_{space}}{Probability_{thermal}}$$

The probability of reaction used for 4.5 eV atomic oxygen is thought to be .138 (6). The probability of reaction for thermal energy neutrals was calculated as follows:

$$Probability_{thermal} = Probability_{space} \times (\frac{E_{thermal}^{.68}}{E_{space}^{.68}})$$

Resulting in reaction probabilities of .0056 and .0104 for energies of .04 eV and .10 eV respectively. The energy terms come from Ferguson's model (14). The actual total flux is calculated as the sum of the ion flux and the actual neutral flux. The results of these calculations for both the directed and scattered beam arrival configurations are presented (Table II) to estimate the ion representation in the beam and its effect on the mass loss of Kapton.

Table II. Ion Representation in Oxygen Beam

Beam Arrival / Measurement	Directed Arrival (45 cm)	Scattered Arrival (45 cm)
Total Effective Flux (Atoms/cm²•s)	1.45×10^{16}	3.87×10^{15}
Ion Current Density (A/cm²)	1.44×10^{-4}	5.22×10^{-5}
Ion Flux (Ions/cm²•s)	9.00×10^{14}	3.26×10^{14}
Neutral Effective Flux (Atoms/cm²•s)	1.23×10^{16}	3.25×10^{15}
Actual Total Flux (Atoms/cm²•s)	1.64×10^{17}	8.08×10^{16}
Thermal Energy Assumed for Neutrals in Calculation of Actual Flux (eV)	0.1	0.04
Flux Ratio Ions/Actual Total Flux (%)	0.55	0.40
Ratio of Kapton Mass Loss Due to Ions/Total Mass Loss (%)	15	16

The calculations for the ratio of ions to the total flux in the beam serves only as an estimate. The reaction probability of thermal atomic oxygen spans three orders of magnitude depending on the model used (6). The model used for these calculations would tend to estimate high the ion content. In the calculations, it was assumed that all the species present were atomic and the ions were singly charged. This along with the fact that many of the neutrals may be present at excited states, makes its difficult to accurately determine the ion to actual flux ratio, though the calculations performed were simple, they are conservative in nature and should provide an upper limit on the ion content. The most important observation that can be made from

11

these calculations is the contribution of mass loss due to ion reaction. These calculations were based on actual mass loss measurements, erosion yields calculated for energies above thermal, and are independent of the reaction probability at thermal energies. These results provide a valuable insight into the actual role that the ions play in the erosion process of Kapton. The ions in the oxygen beam produced by the ECR plasma source contribute only slightly to the mass loss of Kapton, a very reactive material in atomic oxygen. With the ions being at low energies, the material erosion is a chemical process with no threat of physical sputtering. The resulting ratio of ion flux to actual total flux typifies that which occurs in the actual LEO environment.

The ECR plasma source provides the facility accelerated AO testing capabilities based on Kapton effective flux measurements. Though the beam constituents may not be of the same kinetic energy and state as the atomic oxygen in the LEO environment, testing of materials with erosion yields known for in-space exposure provides the most accurate results based on effective flux measurements. For materials with unknown in-space erosion, a Kapton witness or other well characterized reference must be exposed simultaneous with the test subject to provide a reference equivalent flux. Though the use of a reference witness may introduce error in the determination of the total equivalent level of exposure for the test material, since erosion yield is material dependent, it is the simplest (and cost efficient) way to determine the effective fluence for the exposure test.

5. CONCLUDING REMARKS

The LEO atomic oxygen environmental simulation facility provides the capability to evaluate the performance of materials to two of the most damaging factors in the LEO environment, atomic oxygen and VUV radiation. The utilization of an ECR plasma source provides a low energy oxygen beam and deuterium lamps provide VUV radiation. The addition of a reflectance measurement system allows for in situ optical property characterization of test samples while remaining under vacuum. Additional features such as sample heating and articulation are available. Kapton effective flux acceleration factors of 9 to 122 were determined for LEO ram at Space Station Freedom altitudes and the ions present in the beam are of low energy and number. The size of the vacuum chamber combined with the large exposure area provides the ability to evaluate large test samples including functional components. Further evaluation of the VUV intensity in the ECR would be valuable.

The LEO Atomic Oxygen Environmental Simulation Facility at NASA LeRC has been developed in-house with support from Sverdrup Technology, Inc. support service contractors. This facility is utilized extensively by NASA LeRC and its contractors in the evaluation of space power system component materials for Space Station Freedom. The success of Space Station Freedom and other missions operating in the LEO environment will depend on environmental durability evaluations that lead to the selection of durable materials for spacecraft design.

6. REFERENCES

1. J.A. Dever, "Low Earth Orbital Atomic Oxygen and Ultraviolet Radiation Effects on Polymers," NASA Technical Memorandum 103711, February 1991.

2. NOAA, NASA, and USAF, U.S. Standard Atmosphere, 1976, NASA TMX-74335, 1976, pp. 12-15.

3. J.T. Visentine and L.J. Leger, "Material Interactions With the Low Earth Orbital Environment: Accurate Reaction Rate Measurements," JPL Publication 87-14, pp. 11-20, November 1986.

4. B. Banks, et.al., "Neutral Atomic Oxygen Beam Produced by Ion Charge Exchange for Low Earth Orbital Simulation," JPL Publication 87-14, pp. 127-134, November 1986.

5. B.A. Banks, et.al., "Simulation of the Low Earth Orbital Atomic Oxygen Interaction With Materials by Means of an Oxygen Ion Beam," NASA Technical Memorandum 101971, February 1989.

6. B.A. Banks, et.al, "Atomic Oxygen Durability Evaluation of Protected Polymers Using Thermal Energy Plasma Systems" (Paper for presentation at the International Conference of Plasma Synthesis and Processing of Materials, Denver, Colorado, 21-25 February 1993).

7. Features of ECR Plasma Sources, Applied Sciences and Technology, Inc., Woburn, Massachusetts.

8. L. Borget, personal communication, Applied Sciences and Technology, Inc., 15 January 1993.

9. H.R. Kaufman and R.S. Robinson, Operation of Broad Beam Sources, Commonwealth Scientific Corporation, Alexandria, Virginia, 1987, pp. 63-65.

10. S. Samukawa, et.al., Japanese Journal of Applied Physics, 29, (12), L2319, (1990).

11. H.S. Rauschenbach, Solar Cell Array Design Handbook, Van Nostrand Reinhold Co., New York, 1980, pp. 411-12.

12. S.L. Koontz, K. Albyn, and L.J. Leger, Journal of Spacecraft and Rockets, 28,(3), 315, (1991).

13. J.A. Dever and E.J. Bruckner, "The Effects of RF Plasma Ashing on Zinc Orthotitanate/Potassium Silicate Thermal Control Coatings," AIAA Paper No. 92-2171-CP, April 1992.

14. D.C. Ferguson, "The Energy Dependence And Surface Morphology Of Kapton Degradation Under Atomic Oxygen Bombardment," 13th Space Simulation Conference, pp. 205-221, October 1984.

13

REPORT DOCUMENTATION PAGE

Public reporting burden for this collection of information is estimated to average 1 hour per response, including the time for reviewing instructions, searching existing data sources, gathering and maintaining the data needed, and completing and reviewing the collection of information. Send comments regarding this burden estimate or any other aspect of this collection of information, including suggestions for reducing this burden, to Washington Headquarters Services, Directorate for Information Operations and Reports, 1215 Jefferson Davis Highway, Suite 1204, Arlington, VA 22202-4302, and to the Office of Management and Budget, Paperwork Reduction Project (0704-0188), Washington, DC 20503.

1. AGENCY USE ONLY (Leave blank)	2. REPORT DATE May 1993	3. REPORT TYPE AND DATES COVERED Technical Memorandum	
4. TITLE AND SUBTITLE Low Earth Orbital Atomic Oxygen Environmental Simulation Facility for Space Materials Evaluation			**5. FUNDING NUMBERS** WU–474–46–10
6. AUTHOR(S) Curtis R. Stidham, Bruce A. Banks, Thomas J. Stueber, Joyce A. Dever, Sharon K. Rutledge, and Eric J. Bruckner			
7. PERFORMING ORGANIZATION NAME(S) AND ADDRESS(ES) National Aeronautics and Space Administration Lewis Research Center Cleveland, Ohio 44135–3191			**8. PERFORMING ORGANIZATION REPORT NUMBER** E–7797
9. SPONSORING/MONITORING AGENCY NAME(S) AND ADDRESS(ES) National Aeronautics and Space Administration Washington, D.C. 20546–0001			**10. SPONSORING/MONITORING AGENCY REPORT NUMBER** NASA TM–106128

11. SUPPLEMENTARY NOTES

Prepared for the 38th International SAMPE Symposium and Exhibition, sponsored by the Society for the Advancement of Material and Process Engineering, Anaheim, California, May 10–13, 1993. Curtis R. Stidham and Thomas J. Stueber, Sverdrup Technology, Inc., Lewis Research Center Group, Brook Park, Ohio 44142; Bruce A. Banks, Joyce A. Dever, and Sharon K. Rutledge, Lewis Research Center; and Eric J. Bruckner, Cleveland State University, Cleveland, Ohio 44115. Responsible person, Curtis R. Stidham, (216) 433–2299.

12a. DISTRIBUTION/AVAILABILITY STATEMENT Unclassified - Unlimited Subject Category 23	12b. DISTRIBUTION CODE

13. ABSTRACT (Maximum 200 words)

Simulation of low Earth orbit atomic oxygen for accelerated exposure in ground-based facilities is necessary for the durability evaluation of space power system component materials for Space Station Freedom (SSF) and future missions. A facility developed at the National Aeronautics and Space Administrations's (NASA) Lewis Research Center provides accelerated rates of exposure to a directed or scattered oxygen beam, vacuum ultraviolet (VUV) radiation, and offers in-situ optical characterization. The facility utilizes an electron-cyclotron resonance (ECR) plasma source to generate a low energy oxygen beam. Total hemispherical spectral reflectance of samples can be measured in situ over the wavelength range of 250 to 2500 nm. Deuterium lamps provide VUV radiation intensity levels in the 115 to 200 nm range of three to five equivalent suns. Retarding potential analyses show distributed ion energies below 30 electron volts (eV) for the operating conditions most suited for high flux, low energy testing. Peak ion energies are below the sputter threshold energy (~30 eV) of the protective coatings on polymers that are evaluated in the facility, thus allowing long duration exposure without sputter erosion. Neutral species are expected to be at thermal energies of approximately .04 eV to .1 eV. The maximum effective flux level based on polyimide Kapton mass loss is 4.4×10^{16} atoms/cm^2•s, thus providing a highly accelerated testing capability.

14. SUBJECT TERMS Atomic oxygen; Environmental simulation; Electron-cyclotron resonance			15. NUMBER OF PAGES 14
			16. PRICE CODE A03
17. SECURITY CLASSIFICATION OF REPORT Unclassified	18. SECURITY CLASSIFICATION OF THIS PAGE Unclassified	19. SECURITY CLASSIFICATION OF ABSTRACT Unclassified	20. LIMITATION OF ABSTRACT

NSN 7540-01-280-5500

FOURTH CLASS MAIL

ADDRESS CORRECTION REQUESTED

NASA